Sub-10 nm electron beam lithography using cold development of poly(methylmethacrylate)

Wenchuang (Walter) Hu
Department of Electrical Engineering, University of Notre Dame, Notre Dame, Indiana 46556

Koshala Sarveswaran and Marya Lieberman
Department of Chemistry and Biochemistry, University of Notre Dame, Notre Dame, Indiana 46556

Gary H. Bernstein[a)]
Department of Electrical Engineering, University of Notre Dame, Notre Dame, Indiana 46556

(Received 18 December 2003; accepted 26 April 2004; published 30 June 2004)

We investigate poly(methylmethacrylate) (PMMA) development processing with cold developers (4–10 °C) for its effect on resolution, resist residue, and pattern quality of sub-10 nm electron beam lithography (EBL). We find that low-temperature development results in higher EBL resolution and improved feature quality. PMMA trenches of 4–8 nm are obtained reproducibly at 30 kV using cold development. Fabrication of single-particle-width Au nanoparticle lines was performed by lift-off. We discuss key factors for formation of PMMA trenches at the sub-10 nm scale. © *2004 American Vacuum Society.* [DOI: 10.1116/1.1763897]

I. INTRODUCTION

Because the ultimate resolution of electron beam lithography (EBL) can be below 10 nm, and due to its high flexibility, compatibility, and availability, EBL is an important patterning method for nanosystems and devices, such as Coulomb blockade devices,[1–3] molecular electronics,[4,5] high-density magnetic storage,[6] mold making for nanoimprint lithography,[7] and high-precision mask making,[8] among others. During the last four decades, many systems have been developed and processing techniques explored to achieve sub-10 nm fabrication resolution. Some of these techniques use membrane substrates;[9] direct writing on inorganic materials such as NaCl, silicon dioxide,[9] and lithium fluoride films;[10] ultrasonic development;[11] ionized metal evaporation for lift-off;[12] ultra-thin Au film (<2 nm) deposition;[13] system with cold field emitter and isopropyl alcohol (IPA) developer;[14] or Schottky emitter at 100 kV;[15] and novel resist/developer systems.[16,17] EBL, which is a relatively old patterning method, remains perhaps the most useful patterning technique in nanofabrication. As EBL patterning resolution approaches the molecular region (less than 5 nm) with the availability of improved systems, the key issues now are the properties of the resist and developer combination and pattern transfer.[9]

Poly(methylmethacrylate) (PMMA) remains the highest-resolution organic EBL resist used for nanofabrication. Recently, some resists with good etch resistance, such as hydrogen silsesquioxane or HSQ[16] and ZEP (Nippon Zeon Co.),[17] have demonstrated resolution close to 10 nm. We intend to use sub-10-nm-wide PMMA trenches for nanoparticle and molecular lift-off processes for applications in molecular quantum-dot cellular automata (QCA).[5,18] For EBL as a patterning method for molecular QCA by lift-off,[19,20] PMMA still offers ultrahigh resolution and ease of processing.

Nanoparticle patterning has potential for applications in Coulomb blockade devices.[21,22] Patterning resolution, the quality of narrow lines, cross-sectional shape, and absence of residue at the bottom of trenches are critical for successful lift-off. To satisfy these requirements, we are exploring an EBL process with thin PMMA resist using lower-temperature development. Rooks *et al.*[23] and Pantenburg *et al.*[24] have reported that decreasing temperature during development of thick (several micron) PMMA films enhances contrast significantly and achieves better-quality microstructures. However, neither explored the effects of cold development on the resolution of EBL at the nanometer scale, where thin (less than 100 nm) PMMA resist is used. We report here on the effects of development temperatures using atomic force microscopy (AFM) metrology[25–27] and scanning electron microscopy (SEM) on dose requirements, resolution, pattern roughness, trench residue, and cross-sectional shapes in the nanometer regime. Our results show that decreasing the development temperature does not significantly affect contrast for thin resist films, but is found to decrease the sensitivity of PMMA to the developer, which proves to have positive repercussions for sub-10 nm lithography. We found that the combination of using higher doses and cold development improves pattern quality, removes PMMA residue thoroughly, and provides sub-10 nm EBL resolution. Our dose-exposure curves indicate that low-temperature development results in a shorter ''tail'' past the critical dose (CD) on the developer curve, contributing to higher resolution.

II. PROCEDURE

We used a Hitachi S-4500 cold cathode field emission (CCFE) SEM converted to perform beam raster writing[28] with a custom pattern generator.[29] A high-speed beam blanker[30] was installed in the SEM. System noise was re-

[a)]Electronic mail: Bernstein.1@nd.edu

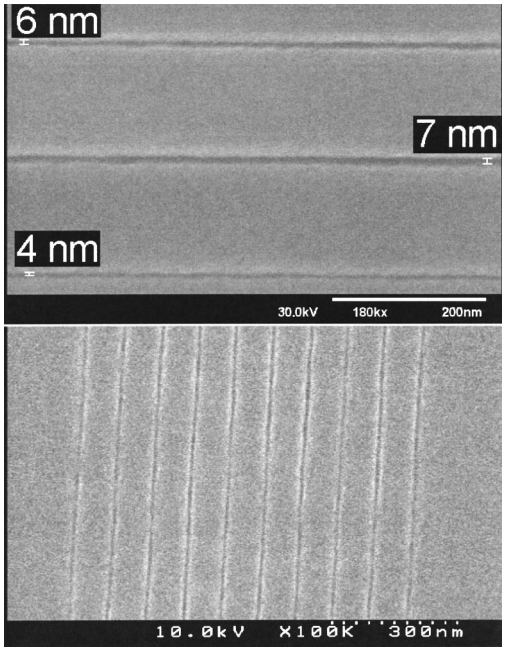

FIG. 1. Intrinsic resolution of EBL on 60-nm-thick PMMA by cold cathode field emission (CCFE) EBL system at 30 kV with development at 6 °C for 30 s. 4-nm-wide and 6-nm-wide lines are shown at top. 6–10-nm-width grating lines are shown at bottom. Line dose is $1.2–1.3\times10^{-9}$ C/cm. Samples are sputter-coated with 1 to 2 nm Cr.

duced by isolating noise sources and eliminating electrical ground loops. A similar EBL system has been reported by Dial *et al.*[14] using nearly the same SEM.

Thin PMMA films were spin-coated onto silicon samples covered with native oxide. The molecular weight of PMMA used was 950 K amu and the thickness was 30–80 nm. Samples were baked at 175 °C in an oven for more than 5 hours, and also baked at 180 °C for 3 min on a hot plate just prior to exposure. EBL was performed at 30 kV with a spot size of 1 to 2 nm, as determined from high-resolution images of sputtered gold on carbon. IPA: Methyl isobutyl ketone (MIBK) (3:1) with 1.5 vol % methyl ethyl ketone (MEK) was used as developer because of its high contrast.[31,32] During development, 10 ml of developer was maintained at a temperature of 4–8 °C with a precision of 1 °C. The 0.5 cm^2 samples were initially at room temperature (around 23 °C). Development time was varied from 7 to 90 s depending on the resist thickness, developer temperature, and exposure dose. Typically, development time was longer for lower doses, lower temperatures, and thicker films.

For SEM examination, either 1- to 2-nm-thick Cr was sputtered on the samples by a plasma sputter coater (Emitech model 675), or 1- to 2-nm-thick AuPd was deposited by thermal evaporation.

III. EXPERIMENTS AND RESULTS

A. Resolution: 4–8 nm PMMA trenches

By using a cold development process, we have reproducibly obtained PMMA trenches narrower than 10 nm, as shown in Fig. 1. Linewidths were measured by our calibrated SEM measurement function and SEMICAPS[33] image-capture system. The system was calibrated with a certified sample[34] with 0.5% accuracy. The lines with 4–8 nm width were clearly resolved without evident microbridging effects, which have been observed for EBL lines narrower than 10 nm.[9,27] We studied the linewidth vs dose at different temperatures. Figure 2 shows that development temperature plays a significant role in determining trench linewidth. With the same developer and dose, colder developer results in narrower linewidths than room temperature. As for the same linewidth, colder developer relates to a 2 to 3 times higher dose. For high-density patterning, a line grating of 40 nm PMMA with 28–30 nm pitch and 5–7 nm linewidths is shown in Fig. 3. Gratings with smaller periods failed due to the collapse of soft PMMA walls.[35]

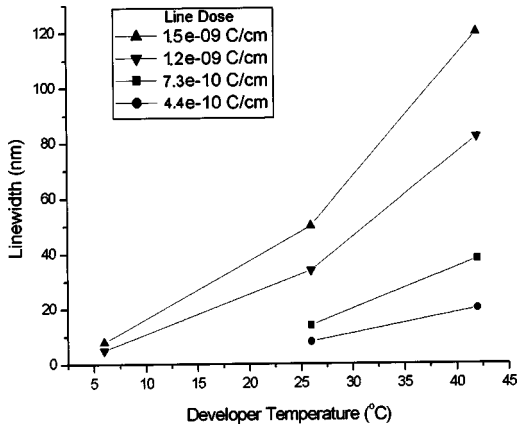

FIG. 2. Linewidth vs developer temperature at different line doses. Developer used in these experiments was IPA:MIBK:MEK 3:1:1.5%. For the same dose, higher developer temperature led to larger final linewidth.

B. Lift-off for Au nanoparticle patterning

Au nanoparticle patterns defined by EBL can potentially be used for multiple-junction single electron transistors and memory.[36] Griffith *et al.*[37] reported direct writing on nanoparticle films to form patterns for blockade devices. A lift-off

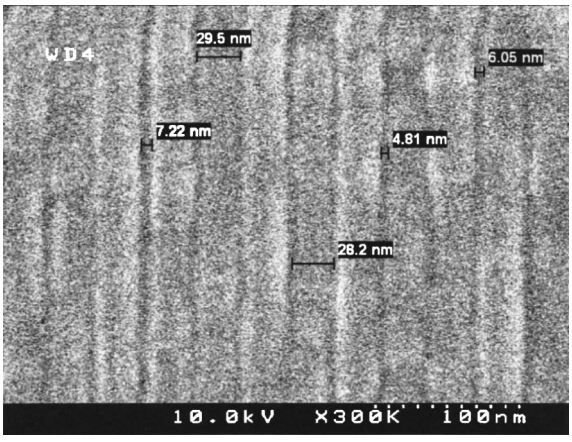

FIG. 3. SEM image of 5–7-nm-wide PMMA grating lines with 28–30 nm pitch. 40-nm-thick PMMA was coated with 1 nm Cr by sputtering.

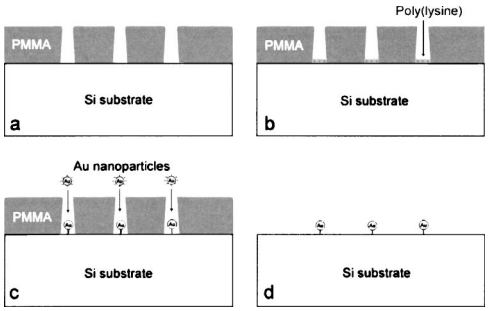

FIG. 4. Schematic diagram of Au nanoparticle attachment and lift-off process. (a) Formation of PMMA trenches by EBL and development at 6 °C; (b) sample soaked in a 0.01 (vol) solution of poly(lysine) for 10 min to make trench bottom positively charged; (c) Au-particle attachment for 10–20 hours; (d) PMMA removal by acetone or 2-dichlorobenzene, leaving the lift-off patterns of Au nanoparticles.

process for Au nanoparticle patterning is presented here. The PMMA trenches were soaked in a solution of poly(lysine) and then exposed to a suspension of citrate-stabilized gold nanoparticles,[38] as illustrated schematically in Fig. 4. The average diameter of the Au nanoparticles was 5.7 nm as measured by transmission electron microscopy (TEM). The PMMA removal was by 2-dichloroethane.[39] Lift-off patterns after EBL and low-temperature development are shown in Fig. 5. Since the Au nanoparticles do not attach to PMMA residue, we conclude that the trench bottom is clear after low-temperature development and that development completely through the resist is successful. As shown in Fig. 5(b), we have demonstrated a Au nanoparticle line with width of one particle. The comparison between Figs. 5(a) and 5(b) shows that wider lines result in multiple-dot-width features, whereas Fig. 5(b) is only one dot wide. This is further evidence that the trench remains narrow to the surface of the substrate, even in the presence of some expected undercut due to both primary and backscattered electron scattering. In the presence of significant undercut, the gold particles would flow to the edges of the trench[19] and reveal a line-width greater than that apparent in the surface SEM micrographs, at least to the resolution of the width of one nanoparticle.

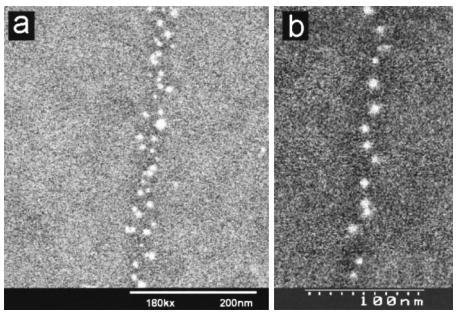

FIG. 5. Lift-off patterns of Au nanoparticles show the patterns were fully developed. (a) Multiple-particle-width line; (b) single-particle-width line.

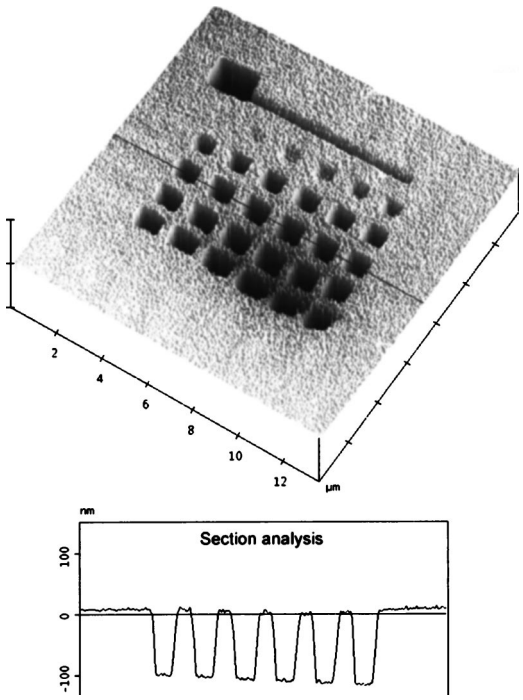

FIG. 6. AFM image of exposed PMMA patterns used to measure contrast. Cross-sectional analysis shows that the roughness of developed squares is maintained at 2%.

C. Contrast measurement by AFM

In order to better understand our results, we performed a study of cold development using AFM metrology.[26,27] We determined the contrast of PMMA resist developed at several different temperatures by measuring the depths of exposed squares with graduated doses. In order to minimize measurement errors, we decreased the pixel spacing in the exposure pattern generator to 1 nm and defocused the beam slightly so that the roughness of the feature bottom is minimized to 0.5–2 nm depending on the dose. Roughness is relatively high in squares with doses close to the critical dose. Figure 6 shows an AFM image and cross-sectional profile of the exposed squares. Roughness of the exposed squares is less than 2% of the resist thickness. The resulting dose-exposure contrast curve is shown in Fig. 7.

The contrast curves in Fig. 7 do not reveal significant differences in contrast between different development temperatures. Instead, we note that temperature affects the sensitivity and, therefore, for a given dose, the intrinsic linewidth. Rooks *et al.*[23] have found that cooling the developer increases contrast significantly while sacrificing sensitivity. For their case, thick (several micron) PMMA films were used for microstructure fabrication by x-ray lithography and loss of sensitivity due to colder developer is not tolerable. However, for the case of thin films and molecular-scale patterning, loss of sensitivity caused by cold development instead allows the use of higher doses, leading to improved pattern quality and higher resolution. Our results agree with theirs on the improvement of pattern quality using cooled developers. Later in this article we discuss the tail shapes of the

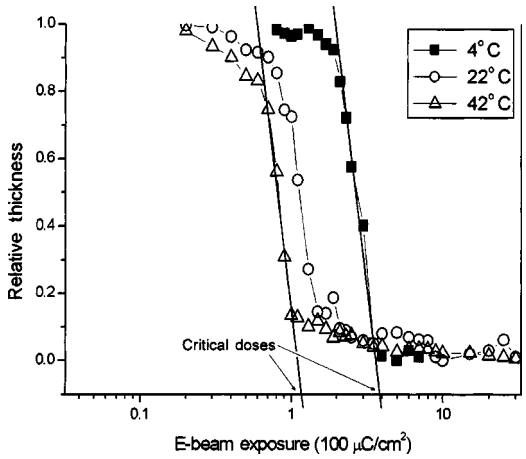

FIG. 7. Development contrast at three different temperatures measured by AFM.

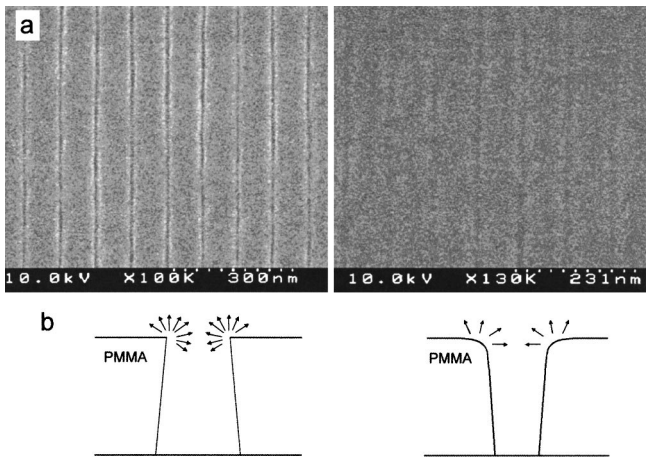

FIG. 8. Comparison of 10-nm-wide intrinsic PMMA lines, (a) developed at 6 °C (left) and 26 °C (right). The doses for the left and right lines were 1.2×10^{-9} C/cm and 4.4×10^{-10} C/cm, respectively. (b) Cartoon explaining how the shape of trench edge affects the contrast. Samples were sputter-coated with 2 nm Cr.

contrast curves at different temperatures and the effect on resolution.

IV. DISCUSSION

Our experimental results demonstrate that low-temperature development enables the fabrication of sub-10 nm structures with a CCFE system at 30 kV. It is useful to understand how cold development affects some key issues of high-resolution EBL, such as resolution, resist residue, pattern quality, and cross-sectional shapes.

A. Resolution

With high-resolution systems, which have either high accelerating voltages (higher than 50 kV), bright small beams (less than 2 nm), or both, the intrinsic resolution of EBL is affected by the combination of dose, resist-developer system, and developer temperature. Based on our experimental results, to fabricate the narrowest PMMA trenches we can use either the lowest possible dose and develop at room temperature (normal EBL process), or use a higher dose but develop at lower temperature (our cold development process). In order to compare both processes, we need to specify the requirements: high spatial resolution, clean trench bottom for lift-off, high trench quality such as low line edge roughness (LER) and sharp cross-sectional shapes.

Chen and Ahmed[11] have reported EBL resolution below 10 nm. They used low doses and room-temperature development and claimed that their ultrahigh resolution was due to the use of ultrasonic agitation during development to help the removal of degraded molecules. Again, using ultrasonic development, Vieu *et al.*[13] reported fabrication of sub-10 nm wide metal lines by lift-off. Ultrasonic agitation was also found to be helpful in cleaning the exposed resist at micron scales.[23] However, the results we obtained from our system using room-temperature development with ultrasonic agitation were not as good as those using low-temperature development without ultrasonic agitation. Their results may be also due to their high-energy (80–200 kV) system with small beam size (<5 nm).

Instead, for our cold development process, during exposure we use a higher dose (2 to 3 times higher) to decrease further and more uniformly the average fragmented molecular weight M^* of the PMMA according to[26]

$$1/M^* = 1/M + gD/\rho N_A, \tag{1}$$

and thereby reduce the residue. Here, M is the original molecular weight of PMMA, D is dose, N_A is Avogadro's number, g indicates the number of effective scissions per unit of deposited energy, and ρ is the density of PMMA. Since M^* decreases rapidly with increasing dose[26] in the low-dose range for high resolution, the higher dose offered by cold development results in lower M^* than room temperature. During cold development, due to the reduction of sensitivity, only the center part of the exposed region is removed by the developer, resulting in sub-10 nm lines. Clean trench bottoms are ensured with high-dose exposure, as demonstrated by the nanoparticle lift-off.

The ''tail'' shapes of the contrast curves in Fig. 7 are important for high resolution. For cold development, the higher dose and lower sensitivity result in a shorter tail on the developer curve past the critical dose, D_f, so that the required dose to actually clear the bottom of the trench lies closer to D_f. Because of this, the minimum deposited energy to clear the trench is more narrowly confined to the center of the trench near the primary beam.

B. Pattern quality

Another issue is the pattern quality, such as cross-sectional shape and LER. The following experiment compares the quality of PMMA trenches of the same width, but developed at different temperatures. Two sets of exposures were performed with the same exposure parameters, PMMA resist preparation, and Cr thickness. The exposed patterns were gratings with graded doses. One sample was developed at 26 °C for 10 s and another at 6 °C for 30 s, which is the

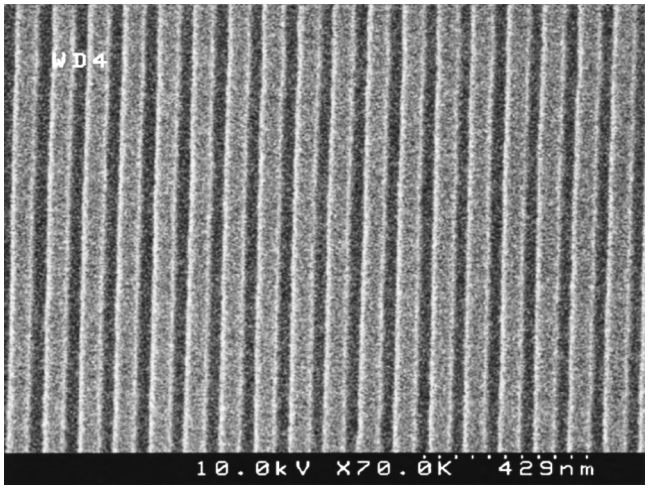

FIG. 9. SEM image of a line grating with sub-30-nm width showing improved LER. The linewidth variation is less than 5 nm after lithography with high dose and cold development. Sample was deposited with 2 nm $Au_{60}Pd_{40}$ by thermal evaporation.

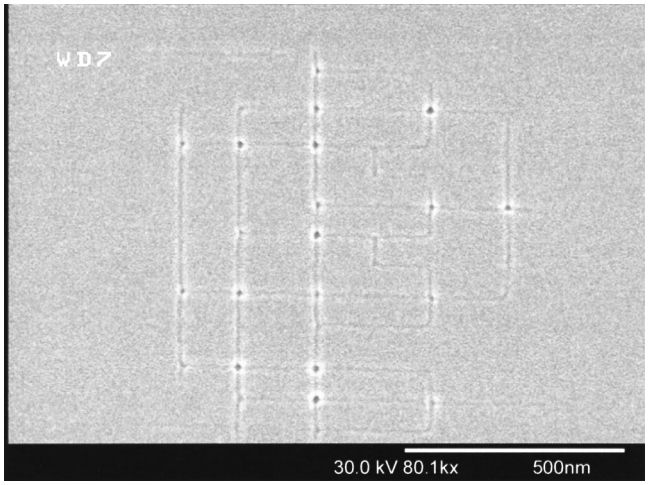

FIG. 10. SEM image of a one-bit full-adder pattern defined by EBL and covered with 1-nm-thick Cr using low-temperature development for molecular QCA. The linewidth is 6–8 nm.

minimum development time needed to clear the trench bottom, as discussed in the next section. Then, the two samples were imaged side by side in the S-4500 SEM. Lines with different doses, but with the same 8–10 nm width, are compared in Fig. 8(a). It appears that lines on the left side, developed at 6 °C, were better resolved and show higher contrast on the edges than those developed at room temperature. The image contrast and brightness in both images were automatically adjusted by the SEM to achieve the same average values. Since the exposure and imaging conditions were the same for both samples, we believe the contrast difference is related to the trench shapes. In the formation of a secondary-electron image from the SEM raster scanning on the lines, sharper edges will generate more secondary electrons[40] and result in higher image contrast. Therefore, as illustrated schematically in Fig. 8(b), lines developed at 6 °C apparently have sharper edges. This is similar in nature to the observation of Pantenburg *et al.*[24] that decreasing developer temperature enhanced structure quality to have sharper edges on the micron scale. At lower temperature, PMMA viscosity η is higher according to[41]

$$\eta = Ae^{\Delta E_{\mathrm{Visc}}/KT}, \tag{2}$$

and dissolution rate of PMMA molecules D will be slower according to[42]

$$D = Ae^{-\Delta E_{\mathrm{ad}}/KT}, \tag{3}$$

where A is a diffusion constant and ΔE_{Visc} and ΔE_{ad} are activation energies, which are functions of the PMMA molecular weight. Therefore, during cold development, the loss of PMMA molecules at trench edges will be less than at room temperature. It has also been reported[43] that for the chemically amplified resist NEB-22 (Sumitomo Chemical), cold development enhances cross-sectional shapes.

Another important quality issue is LER, which relates to beam current variation, scan signal noise, dose, exposure pixel spacing, grating pitch, resist reconfiguration during development, and pattern-transfer processing. Dobisz *et al.*[26] reported that with higher dose and larger grating periods, the grating LER is apparently improved. Cold development allows us to use a dose three times higher and therefore, LER should be lower. Higher dose also results in less noise by averaging the beam current variation from the cold field emission cathode. To achieve lower LER, the exposure pixel spacing should be optimized to eliminate resist residue between pixels.[44] Calculations using a double Gaussian exposure model suggest that the exposure pixel spacing should be no larger than the beam diameter, which agrees with the results of Deshmukh *et al.*[44] Figure 9 shows a PMMA line grating with sub-30-nm width after cold development. Linewidth variation is less than 5 nm, which almost meets critical dimension control requirements (3 nm) for industrially predicted sub-50 nm lithography.[45]

C. Dimension control

It is hard to precisely control the final EBL pattern dimensions due to many factors: beam size, focus, exposure dose, developer chemicals, development time, and development temperature. The ultimate intrinsic linewidth is determined by the combination of these factors. As can be seen in Fig. 2, the developer temperature must be precisely controlled to obtain the desired pattern dimensions.

The development time (which is related to exposure dose, developer composition, sample temperature, resist thickness, and PMMA molecular weight) should be sufficient to clear trench bottoms while being as short as possible to create the narrowest linewidth. For the cold development, the dissolution rate is dramatically reduced [according to Eq. (3)] and development time is longer. We added 1.5% MEK in our developer to increase the dissolution rate and to help removal of PMMA residue.[31] We found 30–60 s is the minimum development time needed at 6 °C with PMMA of 40–60 nm thick, compared with 7–15 s at room temperature.

D. Applications

As discussed before, we believe the cold development with high-dose exposure and the developer with some MEK enables us to define and develop high-aspect-ratio, sub-10 nm PMMA trenches. These clean trenches could be used for attachment of QCA molecules and lift-off to pattern QCA molecular circuits. Figure 10 shows a SEM image of a PMMA trench-pattern of a one-bit QCA full adder[46] for molecular attachment and lift-off. The linewidths are 6–8 nm, but much larger at the overlap, indicating that proximity effects are strong on these size scales. The simple techniques we have investigated could be applied where EBL is needed to define sub-10 nm structures, such as room-temperature single electron transistors and memory, molecular electronics, and quantum devices.

V. SUMMARY AND CONCLUSION

We have reported a cold development process to achieve 4–8 nm EBL and lift-off for Au nanoparticle patterning at the conventional beam voltage of 30 kV. To understand our results, we studied the cold development process using AFM metrology. Several issues of sub-10 nm EBL were discussed and an explanation for higher resolution is proposed that incorporates the slower dissolution rate and higher doses. We believe that the techniques presented here will allow us to perform EBL on the scale of molecules.

ACKNOWLEDGMENTS

This work was performed with support of the ONR/DARPA Grant No. N00014-01-1-0658, Intel, and the W. M. Keck Foundation. We thank Qingling Hang, Min Hu, Alexandra Imre, and Minjun Yan for helpful discussions.

[1]L. Guo, E. Leobandung, L. Zhuang, and S. Y. Chou, J. Vac. Sci. Technol. B **15**, 2840 (1997).
[2]W. Chen and H. Ahmed, J. Vac. Sci. Technol. B **17**, 1402 (1997).
[3]I. Amlani, A. Orlov, G. Toth, G. H. Bernstein, C. S. Lent, G. L. Snider, Science **284**, 289 (1999).
[4]US patent 6,128,214, ''Molecular Wire Crossbar Memory,'' Kuekes, Williams, Heath, HP.
[5]M. Lieberman, S. Chellamma, B. Varughese, Y. Wang, C. Lent, G. H. Bernstein, G. Snider, and F. Peiris, Ann. N.Y. Acad. Sci. **960** (Molecular Electronics II) (2002).
[6]R. P. Cowburn and M. E. Welland, Science **287**, 1466 (2000).
[7]S. Y. Chou *et al.*, J. Vac. Sci. Technol. B **15**, 2897 (1997).
[8]H. Kawano, H. Ito, K. Mizuno, T. Matsuzaka, K. Kawasaki, N. Saitou, H. Ohta, and Y. Sohda, J. Vac. Sci. Technol. B **21**, 823 (2003).
[9]A. N. Broers, A. C. F. Hoole, and J. M. Ryan, Microelectron. Eng. **32**, 131 (1996).
[10]W. Langheinrich, B. Spangenberg, and H. Beneking, J. Vac. Sci. Technol. B **10**, 2868 (1992).
[11]W. Chen and H. Ahmed, Appl. Phys. Lett. **62**, 1499 (1993).
[12]W. Chen and H. Ahmed, J. Vac. Sci. Technol. B **13**, 2883 (1995).
[13]C. Vieu *et al.*, Appl. Surf. Sci. **164**, 111 (2000).
[14]O. Dial, C. C. Cheng, and A. Scherer, J. Vac. Sci. Technol. B **16**, 3887 (1998).
[15]M. Kamp, M. Emmerling, S. Kuhn, and A. Forchel, J. Vac. Sci. Technol. B **17**, 86 (1999).
[16]H. Namatsu, Y. Takahashi, K. Yamazaki, T. Yamaguchi, M. Nagase, and K. Kurihara, J. Vac. Sci. Technol. B **16**, 69 (1998).
[17]K. Kurihara *et al.*, Jpn. J. Appl. Phys., Part 1 **34**, 6940 (1995).
[18]C. S. Lent, P. D. Tougaw, W. Porod, and G. H. Bernstein, Nanotechnology **4**, 49 (1993).
[19]Q. Hang, Y. Wang, M. Lieberman, and G. H. Bernstein, Appl. Phys. Lett. **80**, 4220 (2002).
[20]Y. Chen, D. Macintyre, and S. Thomas, J. Vac. Sci. Technol. B **17**, 2507 (1999).
[21]H. Ahmed, J. Vac. Sci. Technol. B **15**, 2101 (1997).
[22]C. S. Wu, C. D. Chen, S. M. Shih, and W. F. Su, Appl. Phys. Lett. **81**, 4595 (2002).
[23]M. J. Rooks, E. Kratschmer, R. Viswanathan, J. Katine, R. E. Fontana, Jr., and S. A. MacDonald, J. Vac. Sci. Technol. B **20**, 2937 (2002).
[24]F. J. Pantenburg, S. Achenbach, and J. Mohr, J. Vac. Sci. Technol. B **16**, 3547 (1998).
[25]J. Griffith, H. M. Marchman, and L. C. Hopkins, J. Vac. Sci. Technol. B **12**, 3567 (1994).
[26]E. A. Dobisz, S. L. Brandow, R. Bass, and L. M. Shirey, J. Vac. Sci. Technol. B **16**, 3695 (1998).
[27]J. M. Ryan, A. C. F. Hoole, and A. N. Broers, J. Vac. Sci. Technol. B **13**, 3035 (1995).
[28]W. Hu, T. Orlov, and G. H. Bernstein, J. Vac. Sci. Technol. B **20**, 3085 (2002).
[29]G. Bazan and G. H. Bernstein, J. Vac. Sci. Technol. A **11**, 1745 (1993).
[30]E. Weltmer, Scanservice Co., Tustin, CA.
[31]G. H. Bernstein, D. A. Hill, and W. P. Liu, J. Appl. Phys. **72**, 4088 (1992).
[32]M. Khoury and D. K. Ferry, J. Vac. Sci. Technol. B **14**, 75 (1996).
[33]SEMICAPS 2000 imaging system, Santa Clara, CA.
[34]Moxtek standard MXS 301CE.
[35]X. Huang, G. Bazan, G. H. Bernstein, and D. A. Hill, J. Electrochem. Soc. **139**, 2952 (1992).
[36]T. Sato, D. G. Hasko, and H. Ahmed, J. Vac. Sci. Technol. B **15**, 45 (1997).
[37]S. Griffith, M. Mondol, D. S. Kong, and J. M. Jacobson, J. Vac. Sci. Technol. B **20**, 2768 (2002).
[38]C. J. Loweth, W. B. Caldwell, X. Peng, A. P. Alivistos, P. G. Schultz, Angew. Chem., Int. Ed. **38**, 1808 (1999).
[39]Q. Hang, D. A. Hill, and G. H. Bernstein, J. Vac. Sci. Technol. B **21**, 91 (2003).
[40]J. I. Goldstein, D. E. Newbury, P. Echlin, D. C. Joy, A. D. Romig, C. E. Lyman, C. Fiori, and E. Lifshin, *Scanning Electron Microscopy and X-Ray Microanalysis: A Text for Biologists, Materials Scientists, and Geologists*, 2nd ed. (Kluwer, Dordrecht, 1992).
[41]Gordon M. Barrow, *Physical Chemistry for the Life Sciences*, 2nd ed. (McGraw-Hill College Div, New York, 1991).
[42]Robert G. Mortimer, *Physical Chemistry*, 2nd ed. (2000).
[43]L. E. Ocola, D. Tennant, G. Timp, and A. Novembre, J. Vac. Sci. Technol. B **17**, 3164 (1999).
[44]P. R. Deshmukh, K. J. Rangra, and O. P. Wadhawan, Vacuum **52**, 469 (1999).
[45]International Technology Roadmap for Semiconductors (2002). http://public.itrs.net/Files/2002Update/Home.pdf
[46]P. D. Tougaw and C. S. Lent, J. Appl. Phys. **75**, 1818 (1994).